

Al-to-Cu Friction Stir Lap Welding

VAHID FIROUZDOR and SINDO KOU

Recently, friction stir welding (FSW) has been used frequently to join dissimilar metals, for instance, Al to Mg, Cu, and steel. The formation of brittle intermetallic compounds often severely limits the strength and ductility of the resultant welds. In the present study, Al-to-Cu lap FSW was studied by welding 6061 Al to commercially pure Cu. Conventional lap FSW was modified by butt welding a small piece of Al to the top of Cu, with a slight pin penetration into the bottom of Al. At travel speeds up to 127 mm/min (5 ipm), the modified welds were about twice the joint strength and five to nine times the ductility of the conventional lap welds. In the conventional lap welds, voids were present along the Al–Cu interface, and fracture occurred along the interface in tensile testing. No such voids were observed in the modified lap welds, and fracture occurred through Cu. Thus, as in the case of Al-to-Mg lap FSW recently studied by the authors, modified lap FSW significantly improved the weld quality in Al-to-Cu lap FSW. At the relatively high travel speed of 203 mm/min (8 ipm), however, modified lap FSW was no longer superior because of channel formation.

DOI: 10.1007/s11661-011-0822-9

© The Minerals, Metals & Materials Society and ASM International 2011

I. INTRODUCTION

JOINING dissimilar materials has been suggested as a top priority in materials joining technology,^[1,2] for instance, Al-to-steel or Al-to-Mg for weight reduction, and Al-to-Cu for electric connections. Recently, friction stir welding (FSW)^[3] has been used to join dissimilar metals by plunging the pin at the bottom of a rotating tool into the workpiece and traversing it along the joint to cause bonding by stirring and mixing them together.

Conventional lap^[4–8] and butt^[9–18] FSW of Al alloys to pure Cu FSW have been investigated frequently. As shown in Table I, in lap FSW, Al has always been put on top. For convenience of discussion, the Al–Cu phase diagram^[19] is shown in Figure 1. According to the phase diagram, when Al and Cu are heated together, several intermetallic compounds can form in the solid state by diffusion, including Al₂Cu. Upon additional heating, liquation (*i.e.*, liquid formation) occurs at 821 K (548 °C) by the Al + Al₂Cu → L reaction.

Elrefaey *et al.*^[5,6] lap welded 2-mm-thick 1100 Al to 1-mm-thick commercially pure Cu. The tool was made of a tool steel. The shoulder was concave and 10 mm in diameter. The pin was 3 mm in diameter, 1.7-mm long, and threaded. The tilt angle was 3 deg. The travel speed ranged from 200 to 300 mm/min and the rotation speed ranged from 1000 to 2500 rpm. The resultant welds were peel tested. The welds failed prematurely before testing

if the pin tip was positioned at 0 mm above Cu, but did not fail if the pin tip penetrated the Cu by 0.1 mm. A dark-etching zone appeared at the interface between 1100 Al and Cu, in which layers of intermetallic compounds existed along the interface and in the Cu-rich fragments nearby in the stir zone. Intermetallic compounds were identified by X-ray diffraction (XRD), including CuAl (η), CuAl₂ (θ), and Cu₉Al₄ (γ). CuAl₂ (θ) appeared black, CuAl (η) appeared gray, and Cu₉Al₄ (γ) appeared layered. In one weld made with a 50- μ m Zn foil inserted between Al and Cu, the strength was significantly higher because, as suggested, Zn possibly reduced the formation of harmful Al_mCu_n.

Abdollah-Zadeh *et al.*^[7,8] lap welded 4-mm-thick 1060 Al to 3-mm-thick commercially pure Cu. The tool was made of a tool steel. The shoulder diameter was 15 mm. The pin was 5 mm in diameter, 6.5-mm long, and threaded. The tilt angle was 3 deg. The resultant welds were tensile tested (shear tensile). The travel speed ranged from 30 to 375 mm/min and the rotation speed ranged from 750 to 1500 rpm. Judging from the transverse macrograph of a weld made at 95 mm/min and 1180 rpm, the pin tip penetrated Cu by 0.2 mm (But the difference between the 6.5-mm pin length and 4-mm thickness of the 1060 Al at the top was 2.5 mm). Cu-rich fragments were found in the stir zone, with intermetallic compounds between the particles and the stir zone. A series of transverse macrographs were taken for welds made at 1180 rpm and various travel speeds. It was shown that, at 118 and 190 mm/min travel speeds, “cavity or groove-like defects” appeared at the interface between 1060 Al and Cu. Citing the study of Kim *et al.*,^[20] the authors attributed this problem to insufficient heat input and hence plastic flow at high travel speeds. At 300 and 375 mm/min, no bonding occurred between 1060 Al and Cu. Intermetallic compounds were identified by energy-dispersive spectroscopy (EDS), including CuAl (η), CuAl₂ (θ) and Cu₉Al₄ (γ).

VAHID FIROUZDOR, formerly Research Assistant, with the Department of Materials Science and Engineering, University of Wisconsin, Madison, WI 53706, is now a Research Assistant with the Department of Engineering Physics, University of Wisconsin. SINDO KOU, Professor, is with the Department of Materials Science and Engineering, University of Wisconsin. Contact e-mail: kou@enr.wisc.edu.

Manuscript submitted August 2, 2010.

Article published online July 20, 2011

Table I. Lap FSW of Al Alloys to Pure Cu

	Top	Bottom	Penetration into Bottom	Welding Parameters
Okamura <i>et al.</i> ^[4]	6061 Al, thickness unspecified	Cu, thickness unspecified	Unspecified	Unspecified
Elrefaey <i>et al.</i> ^[5,6]	1100 Al, 2 mm	Cu, 1 mm	0.1 mm, 0 mm (broke)	1000–2500 rpm 200–300 mm/min
Abodollah-Zadeh <i>et al.</i> ^[7,8]	1060 Al, 4 mm	Cu, 3 mm	~0.2 mm	750–1500 rpm 30–375 mm/min

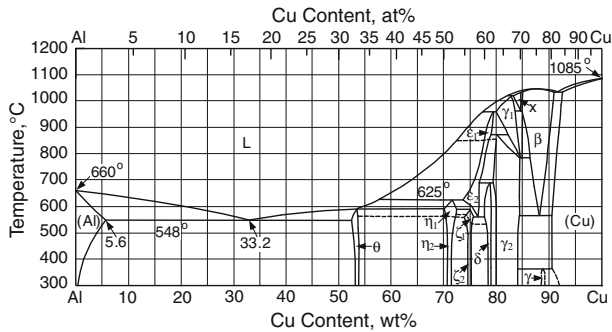


Fig. 1—Al-to-Cu lap welding by FSW: (a) conventional lap FSW; (b) modified lap FSW.

The purpose of the present study is to study lap FSW of Al to Cu. Conventional lap FSW will be conducted. In addition, the modified lap FSW recently proposed by Firouzdar *et al.*^[21,22] will also be attempted. As demonstrated by Firouzdar *et al.*, both the strength and the ductility of Al-to-Mg lap welds can be increased significantly by modifying conventional lap FSW.

II. EXPERIMENTAL PROCEDURE

A. Welding

6061 Al was welded to commercially pure Cu by FSW. Their nominal chemical compositions are listed in

Table II. Coupons were cut from 1.6-mm-thick sheets of 6061-T6 Al alloy and Cu. They were cleaned with a stainless steel brush to remove surface oxides. A Lagun FTV-1 (Republic Lagun, Harbor City, CA) milling machine (2.2 kW or 3 HP) was used for FSW with tools prepared from a H13 tool steel. The tool shoulder was 10 mm in diameter and concave. The pin was 4 mm in diameter and threaded, and the pin length was 1.6 mm. The tool was rotated counterclockwise when viewed from above and tilted 3 deg forward. The work pieces were clamped tight with four steel fingers located 10 mm away from the weld line. The tool was cleaned after each welding pass by plunging it into a fresh piece of 6061 Al to remove material from previous welds. This step was repeated several times until the tool was clean. The travel speed varied from 38 mm/min (1.5 ipm) to 203 mm/min (8 ipm). The rotation speed was 1400 rpm.

Table III summarizes the experimental conditions for the conventional lap (CL) and modified lap (ML) welds made in the present study.

In conventional lap FSW, 6061 Al was placed at the top and Cu was placed at the bottom. The work piece dimensions are shown in Figure 2(a). Lap welding was positioned along the centerline of the 38-mm-wide overlap. In modified lap FSW, however, Cu was placed at the top and 6061 Al was placed at the bottom. The work piece dimensions are shown in Figure 2(b). A small piece of 6061 Al, 76-mm long, 19-mm wide and 1.6-mm thick, was butt welded to the Cu at the top with a slight pin penetration into the bottom sheet, as

Table II. Composition of Work piece Materials (Wt Pct) and Yield and Tensile Strengths

	Si	Cu	Mn	Mg	Cr	Zn	Ti	Fe	Al	Yield Strength (Mpa)	Tensile strength (Mpa)
6061 Al	0.62	0.28	0.08	0.89	0.19	0.02	0.01	0.52	balance	310	280
Cu	—	>99.5	—	—	—	—	—	—	—	275	250

Table III. Experimental Conditions for of the CL and ML Welds

#	Joint	Rotation Speed (rpm)	Travel Speed (mm/min)
CL-1	Al (top) to Cu (bottom)	1400	38
CL-2	Al (top) to Cu (bottom)	1400	76
CL-3	Al (top) to Cu (bottom)	1400	127
CL-4	Al (top) to Cu (bottom)	1400	203
ML-1	Top: Cu (ret) and small Al (adv); Bottom: Cu	1400	38
ML-2	Top: Cu (ret) and small Al (adv); Bottom: Cu	1400	76
ML-3	Top: Cu (ret) and small Al (adv); Bottom: Cu	1400	127
ML-4	Top: Cu (ret) and small Al (adv); Bottom: Cu	1400	203

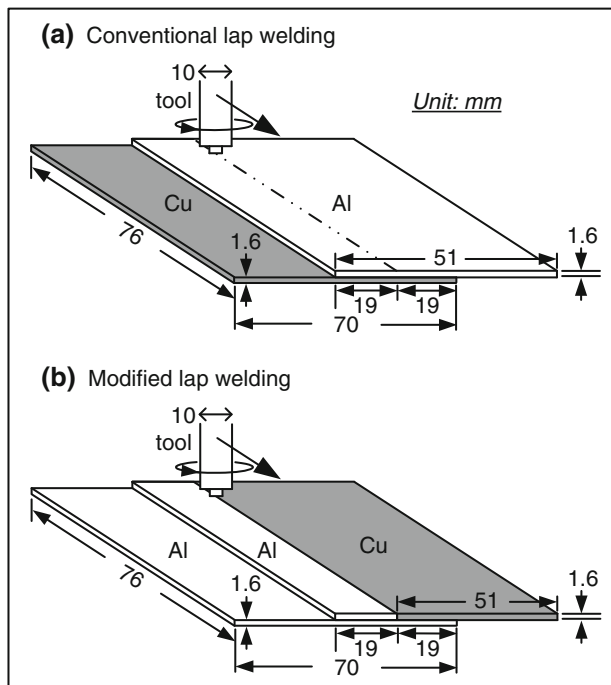


Fig. 2—Binary Al-Cu phase diagram^[19].

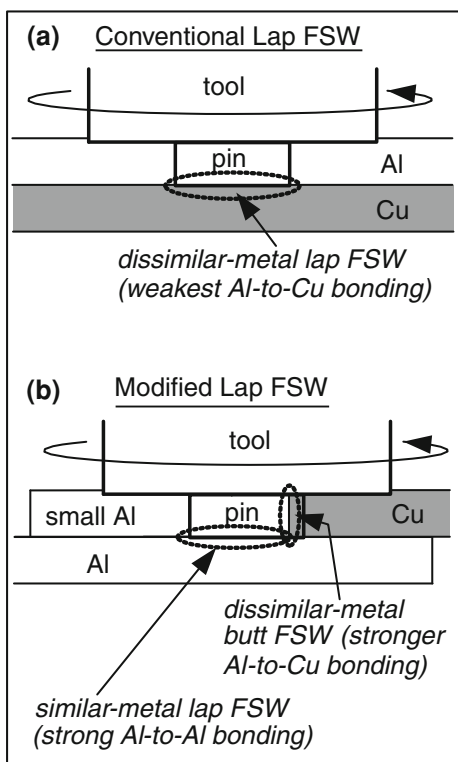


Fig. 3—Lap FSW of Al to Cu: (a) conventional lap; (b) modified lap. Modified lap is achieved by butt welding a small piece of Al to Cu with a slight pin penetration into the bottom of the Al. To maximize strong Al-to-Al bonding, the pin is shifted into Al.

illustrated in Figure 3. The 19-mm width of the small piece was mainly for the space required for clamping instead of welding. The small 6061 Al was placed on the

advancing side of the tool. Figure 4 compares the top view of weld CL-1 with that of weld ML-1. The top surface of weld ML-1 is not as smooth as that of weld CL-1 but it is still acceptable. With Cu on the advancing side, the resultant weld was much worse, even with visual inspection. Perhaps the heat input was too high based on Al-Mg dissimilar FSW by the authors.^[21–24]

B. Tensile Testing

The joint strength was determined by tensile testing normal to the weld. Welded coupons were cut in the direction normal to the weld into 12-mm-wide tensile specimens. The edges of the tensile specimens were polished smooth with 320-grit grinding paper. For lap welds, a 1.6-mm-thick sheet was placed at each end of the tensile specimen to align the specimen with the loading direction. A MTS Sintech (MTS, Eden Prairie, MN) tensile testing machine was used, and the speed of the crosshead movement was 1 mm/min. Two to four specimens from welds made under the same conditions were tested. Elongation of the joint is considered as the strain at the fracture point measured by the crosshead movement of the tensile machine.

C. Weld Microstructure

Transverse weld cross sections were polished and etched in two steps. The first step was to etch the samples with a solution consisting of 10-g iron (III) nitrate in 100 mL of distilled water for 1 minute (to reveal the copper part of the microstructure). The second step was to etch them with a solution consisting of 20-g NaOH + 0.5-g KMnO₄ in 100 mL distilled water for 40 seconds (to reveal the microstructure in 6061 Al). KMnO₄ showed the stir zone in 6061 Al in color.

To study the fracture surfaces, scanning electron microscopy (SEM) was conducted using a Hitachi S3400 (Hitachi High Technology, Europe GmbH, Krefeld, Germany) microscope equipped with EDS. To identify the intermetallic compounds, XRD was conducted on fragments removed from the fracture surface using a D/Max Rapid II X-ray diffractometer (Rigaku Corporation, Tokyo, Japan) equipped with a Mo K α X-ray source. Unlike most X-ray diffractometers, this special equipment allows diffraction in the transmission as well as a reflection mode, which often results in better resolution.

III. RESULTS AND DISCUSSION

A. Tensile Properties

For conventional lap FSW, the joint strength remains essentially constant at about 2 kN and the ductility at about 2.5 pct at all travel speeds, as shown in Figure 5. The joint strength in the present study will be compared with that in the study by Abdollah-Zadeh *et al.*^[7,8] as follows. In the present study, the weld made at 76 mm/min and 1400 rpm failed in tensile testing through the nugget at about 2.2 kN (Figure 5(a)). The most closely

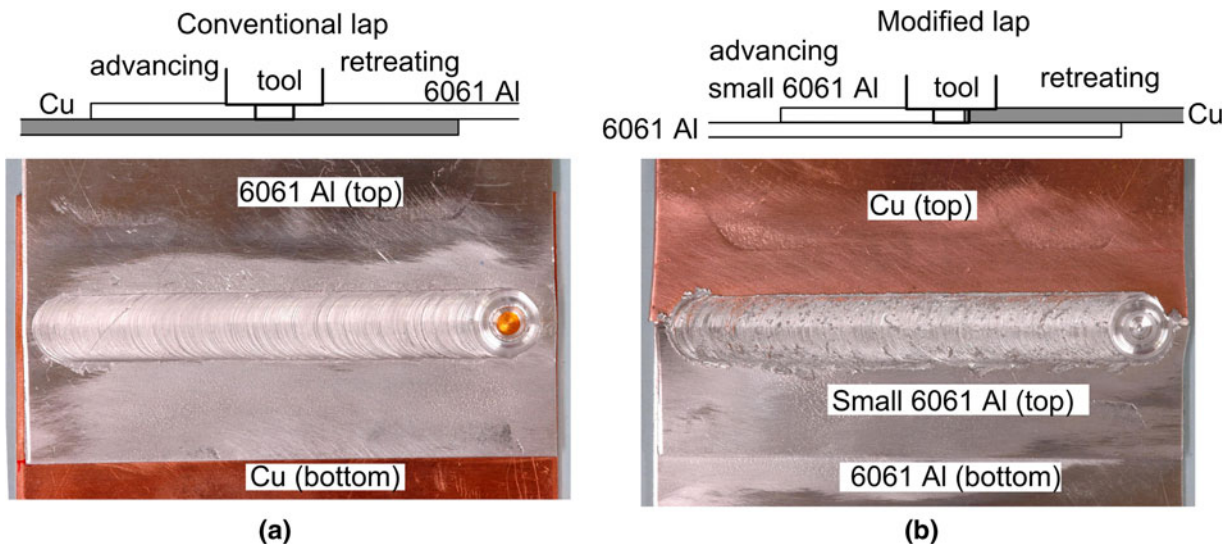


Fig. 4—Top views of Al-to-Cu welds made by (a) conventional lap FSW and (b) modified lap FSW.

related weld in Abdollah-Zadeh *et al.*'s study was the one made at 60 mm/min and 1500 rpm, which failed in tensile testing at 2.152 kN through the nugget. Because the specimen is 12-mm wide in the present study, as opposed to 10 mm in their study, the 2.2 kN of this joint strength is equivalent to 1.83 kN ($= 2.2\text{kN} \times 10/12$) based on a 10-mm specimen width, which is 85 pct of 2.152 kN. However, the tool is significantly smaller in the present study (4-mm pin diameter and 10-mm shoulder diameter) than in their study (5-mm pin diameter and 15-mm shoulder diameter). Because the joint strength increases with increasing bonding area, the joint strength in the present study is likely to be comparable with that in their study. As for the study by Elrefaey *et al.*,^[5,6] peel testing was conducted instead of tensile testing, and thus, no comparison in the joint strength can be made.

The tensile properties of the modified lap welds, however, are much better than those of the conventional ones as shown in Figure 5. At relatively low travel speeds up to 127 mm/min (5 ipm), the modified lap welds were about twice higher in joint strength and five to nine times higher in ductility than the conventional lap welds. Thus, as in Al-to-Mg lap FSW,^[21,22] modified lap FSW can significantly improve the weld quality in Al-to-Cu lap FSW. Figure 6 shows the tensile test curves of the conventional and modified lap welds made at 1.5 ipm (38 mm/min). At the relatively high travel speed of 203 mm/min (8 ipm), however, modified lap welds became close to the conventional ones in joint strength and ductility (Figure 5).

The fracture surfaces of the conventional lap welds show brittle failure along the interface between 6061 Al and Cu. Figure 7 shows the fracture surface of the conventional lap weld CL-1 made at 38 mm/min (1.5 ipm). Figure 8 shows the XRD results of a fragment from the fracture surface similar to the one shown in Figure 7(f). As shown, CuAl_2 (θ) and Cu_9Al_4 (γ) are

identified as the major intermetallic compounds formed in the Al-to-Cu lap welds. However, it is inconclusive as to whether CuAl (η) also exists because the intensity levels at its major diffraction peaks are rather low. As shown in Figure 7(c), fracture initiates from the triple junction between 6061 Al, Cu, and the stir zone and propagates inward along the interface between the stir zone and the Cu before turning upward to cut through the bulk stir zone. EDS analysis confirms the presence of the intermetallic compounds on the fracture surface. Cu patches are also visible on the fracture surface in Figure 7(c). They suggest failure along the interface between the layer of intermetallic compounds near the bottom of the stir zone and the Cu as well as through the layer. The SEM images in Figures 7(d) through (f) show flat fracture surfaces that are typical of brittle failure. The marks left by the rotating pin tip are visible on the fracture surface (Figures 7(e) and (f)). The microstructure of the weld and its intermetallic compounds will be discussed subsequently in Figure 10.

The fracture surfaces of the modified lap welds show ductile failure through Cu. Figure 9 shows the fracture surface of the modified lap weld ML-1 made at 38 mm/min (1.5 ipm). As shown in Figures 9(b) and (c), failure is through Cu and mostly outside the stir zone. The fracture surface in Figure 9(c) shows a white layer of Al-rich material at the top of the Cu. The SEM image in Figure 9(d) shows the fracture surface in an area similar to the boxed area in Figure 9(c). The SEM image in Figure 9(e), corresponding to the top boxed area in Figure 9(d), shows a flat fracture surface that suggests failure through brittle intermetallics. The EDS spectrum of the brittle fracture area in Figure 9(g) shows the presence of both Al and Cu, thus confirming the presence of Al-Cu intermetallic compounds. Conversely, the SEM image in Figure 9(f), corresponding to the bottom boxed area in Figure 9(d), shows clear dimples that suggest ductile fracture through Cu. The final

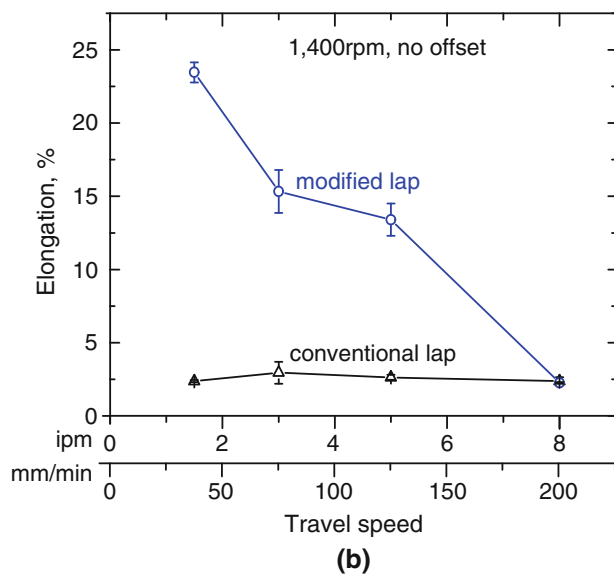
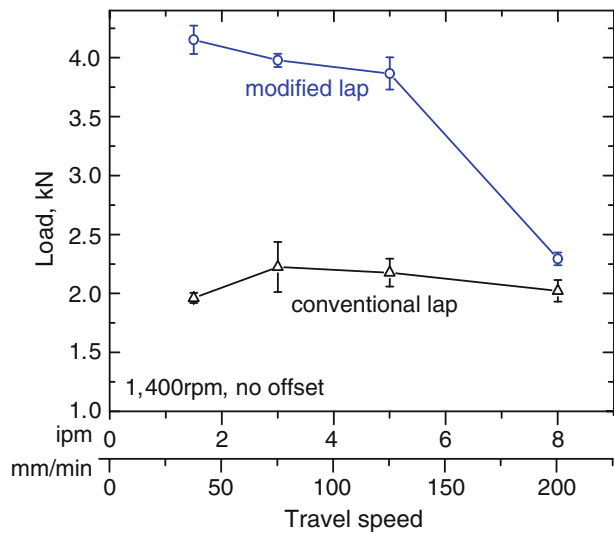


Fig. 5—Strength and ductility of Al-to-Cu lap welds: (a) strength; (b) ductility.

fracture occurs through Cu most likely because cracks have already initiated in Cu through the brittle intermetallic compounds (because it is a softer material with lower tensile strength compared with 6061 Al, as shown in Table II). Figure 9(h) shows the EDS spectrum of a particle inside a dimple in Figure 9(f) that indicates a high O content in the particle, which suggests that it is copper oxide. Oxide particles are present in the dimples because the commercially pure Cu is not oxygen free.

B. Microstructure

The microstructure of the conventional lap welds shows several dark-etching intermetallic compounds and even voids along the interface between the portion of the stir zone in 6061 Al and that in Cu. Presumably, these voids and intermetallic compounds acted as

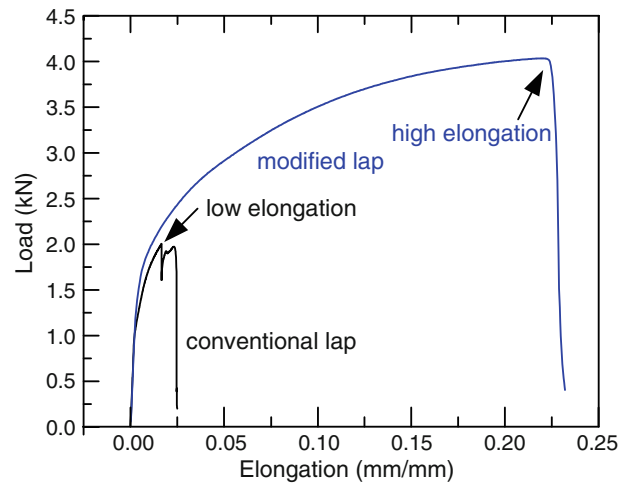


Fig. 6—Tensile test curves of conventional lap weld CL-1 (1.5 ipm or 38 mm/min) and modified lap weld ML-1 (1.5 ipm or 38 mm/min) between 6061 Al and Cu.

fracture initiation sites during tensile testing and reduced the joint strength and ductility.

Figure 10 shows the transverse cross section of the conventional lap weld CL-1 made at 38 mm/min (1.5 ipm). The boundary between the stir zone and the 6061 Al is sharper on the advancing side of the tool (left) than on the retreating side (right). The stir zone (Figure 10(b)) extends through the thickness of 6061 Al into Cu. The portion of the stir zone inside 6061 Al consists of the following regions: (1) a wide light-etching bulk stir zone of essentially 6061 Al at the top, and (2) a much narrower onion-ring structure (Figure 10(b)) at the bottom. The onion-ring structure contains numerous dark-etching Cu-rich particles (Figure 10(c)). The portion of the stir zone inside Cu also consists of the following regions: (1) a darker-etching layered structure at the top (Figures 10(e) and (f)), and (2) a lighter-etching region of stirred and grain-refined Cu (Figure 10(b)).

Figure 11(a) shows the SEM back-scattered electron (BSE) image of the boxed area in Figure 10(b). As shown by the EDS map of Al in Figure 11(b), the bulk stir zone in 6061 Al has a dark red color, which suggests that the Cu is absent. However, the stir zone below it shows a matrix that is lighter red in color. This lighter color perhaps suggests that, in addition to Cu particles, as shown by the EDS map of Cu in Figure 11(c), a solid solution of Al containing some Cu also might be present in the matrix. The SEM BSE image in Figure 11(d) shows the stir zone at a higher magnification. The corresponding EDS map of Cu shown in Figure 11(e) at an even higher magnification suggests an essentially uniform Cu distribution in the matrix of 6061 Al. The EDS measurement of the matrix shows about 3 to 6 wt pct Cu. This is significantly higher than the Cu content in 6061 Al (about 0.4 wt pct Cu), but still within the solubility limit of Cu in Al (5.6 wt pct Cu, according to the Al-Cu phase diagram). The distribution of small Cu particles is also noticeable.

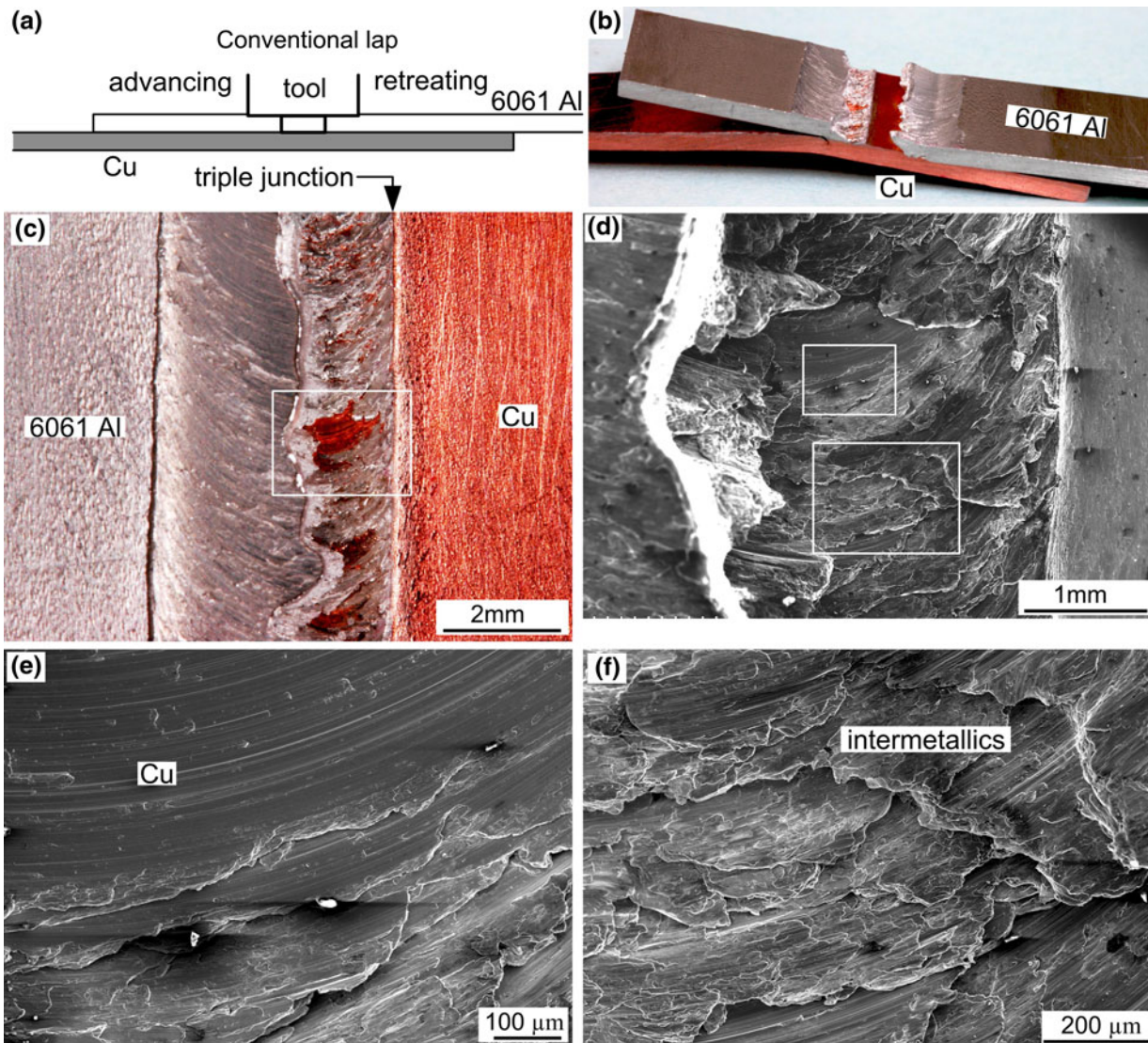


Fig. 7—The fracture surface of conventional lap weld CL-1 (1.5 ipm or 38 mm/min) showing failure along interface between 6061 Al and Cu: (a) joint design; (b) and (c) photographs of the failed specimen; (d) through (f) SEM images of the fracture surface. Fracture initiated from the triple junction among 6061 Al, Cu, and the stir zone.

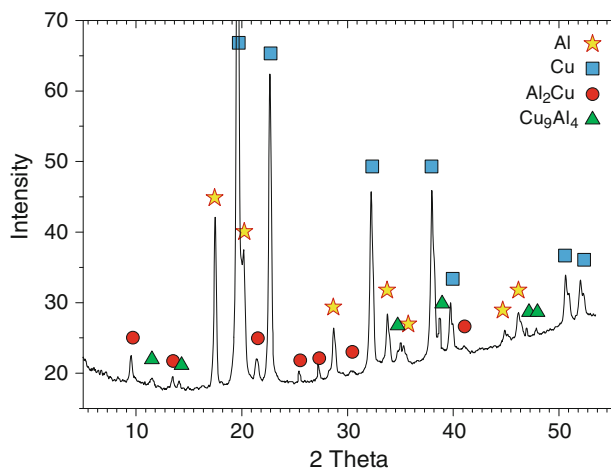


Fig. 8—XRD (transmission mode) of a fragment removed from the fracture surface of weld CL-1 (1.5 ipm or 38 mm/min) shown in Fig. 6.

Several voids are present along the interface between the lower region of the stir zone in 6061 Al and the upper region of the stir zone in Cu. An optical micrograph was taken in the as-polished condition (Figure 10(d)) to reveal the voids clearly. In the etched condition, the areas occupied by voids and some intermetallic materials both appear dark, and it is thus often difficult to tell them apart (Figures 10(e) and (f)). During tensile testing, fracture initiated from the triple junction (Figure 7(c)) among 6061 Al, Cu, and the stir zone on the retreating side, propagating easily through the voids before cutting through the thickness of the bulk stir zone. This explains the relatively low strength and ductility of the weld in tensile testing (Figure 5).

Figure 12 shows the transverse cross section of the conventional lap weld CL-2 made at 203 mm/min (8 ipm). The stir zone (Figure 12(b)) is similar to that of conventional lap weld CL-1 made at a lower travel speed of 38 mm/min (1.5 ipm) (Figure 10(b)). However,

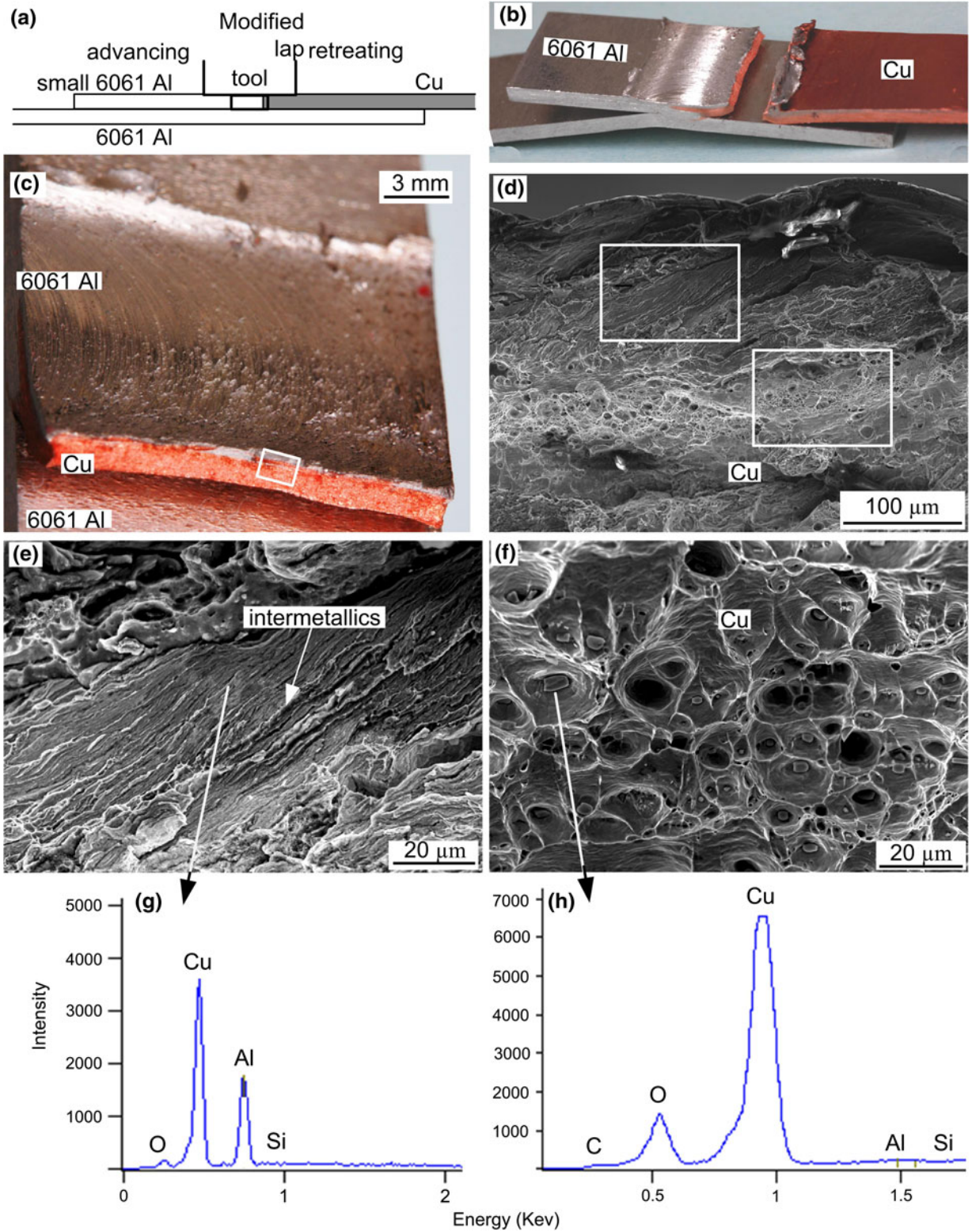


Fig. 9—Fracture surface of conventional lap weld ML-1 (1.5 ipm or 38 mm/min) showing failure through Cu: (a) joint design; (b) and (c) photographs of the failed specimen; (d) through (f) SEM images of the fracture surface; (g) and (h) EDS spectrum from the fracture surface.

the portion of the stir zone inside 6061 Al no longer exhibits an onion-ring structure at the bottom. Instead, the bottom consists of a few Cu-rich particles embedded

in a matrix that etches somewhat light brown in color, which again might suggest the presence of Cu particles and perhaps a solid solution in the matrix. As shown in

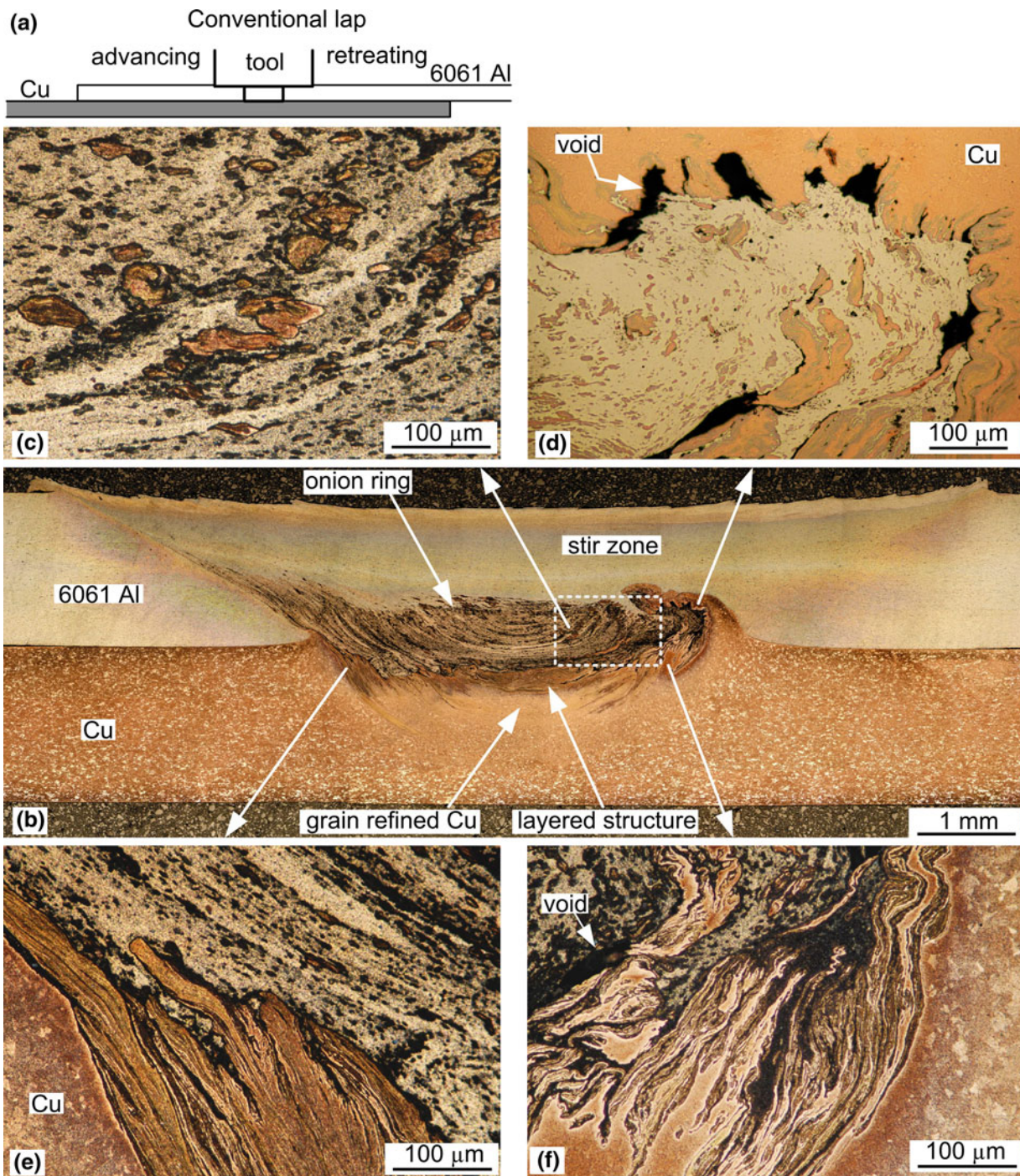


Fig. 10—Transverse cross section of conventional lap weld CL-1 (1.5 ipm or 38 mm/min): (a) joint design; (b) optical macrograph; (c), (e), and (f) etched optical micrographs; (d) as-polished optical micrograph to reveal voids clearly. The boxed area in (b) indicates the location of the SEM BSE image shown in Fig. 10(a).

Figure 12(c), the Cu-rich particles are fewer in number and larger in size = compared with those in Figure 10(c) for the conventional lap weld made at the lower travel speed of 38 mm/min (1.5 ipm). It seems that a significantly faster travel speed discourages the distribution of copper particles inside the stir zone as well as the formation of a clear onion-ring structure. Again, several

voids are present along the interface between the stir zones in 6061 Al and Cu (Figures 12(d) through (f)). The presence of these voids is consistent with the relatively low strength and ductility of the weld in tensile testing (Figure 5).

Figure 13 shows the transverse cross section of the modified lap weld ML-1 made at 38 mm/min (1.5 ipm).

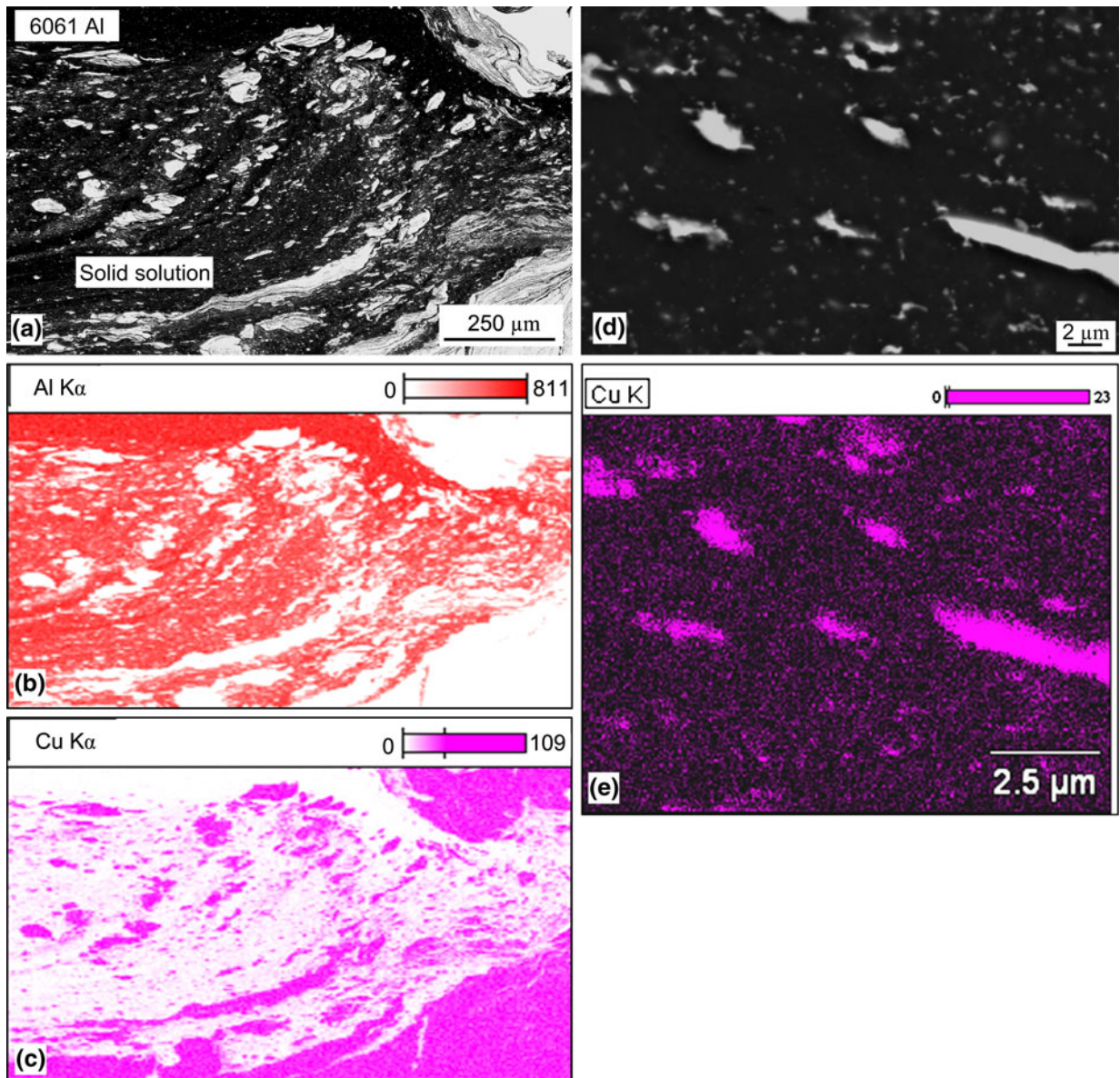


Fig. 11—Distributions of Al and Cu in conventional lap weld CL-1 (1.5 ipm or 38 mm/min) in the boxed area in Fig. 9(b): (a) low-magnification SEM BSE image; (b) EDS map of Al; (c) EDS map of Cu; (d) high-magnification SEM BSE of stir zone; (e) EDS map of Cu in (d).

The stir zone (Figure 13(b)) extends through the thickness of the upper 6061 Al into the lower one. The onion-ring structure is contiguous from the upper 6061 Al to the lower one. This indicates that similar metal bonding between the upper and lower 6061 Al is maximized as illustrated in Figure 3. Under the shearing/peeling action inherent during tensile testing of lap welds, the void can easily open up and lead to premature failure. In weld ML-1, however, Al-to-Al bonding is free of intermetallics and voids and is thus strong. The upper portion of the stir zone in Cu is pulled deep into the stir zone of the upper 6061 Al to interlock with it. No evidence exists of voids or thick intermetallic layers

along the interface between 6061 Al and Cu. Thus, during tensile testing, fracture did not propagate along the interface but through Cu (Figure 9). This finding is consistent with the high strength and ductility of the weld (Figure 5).

Figure 14 shows the transverse cross section of the modified lap weld ML-2 made at 203 mm/min (8 ipm). The stir zone (Figure 14(b)) differs in several ways from that of modified lap weld ML-1 made at a lower travel speed of 38 mm/min (1.5 ipm) (Figure 13(b)). An onion-ring structure still exists in 6061 Al but with coarser spacing between rings. The stir zone in 6061 Al consists of a few large, Cu-rich particles embedded in a matrix that

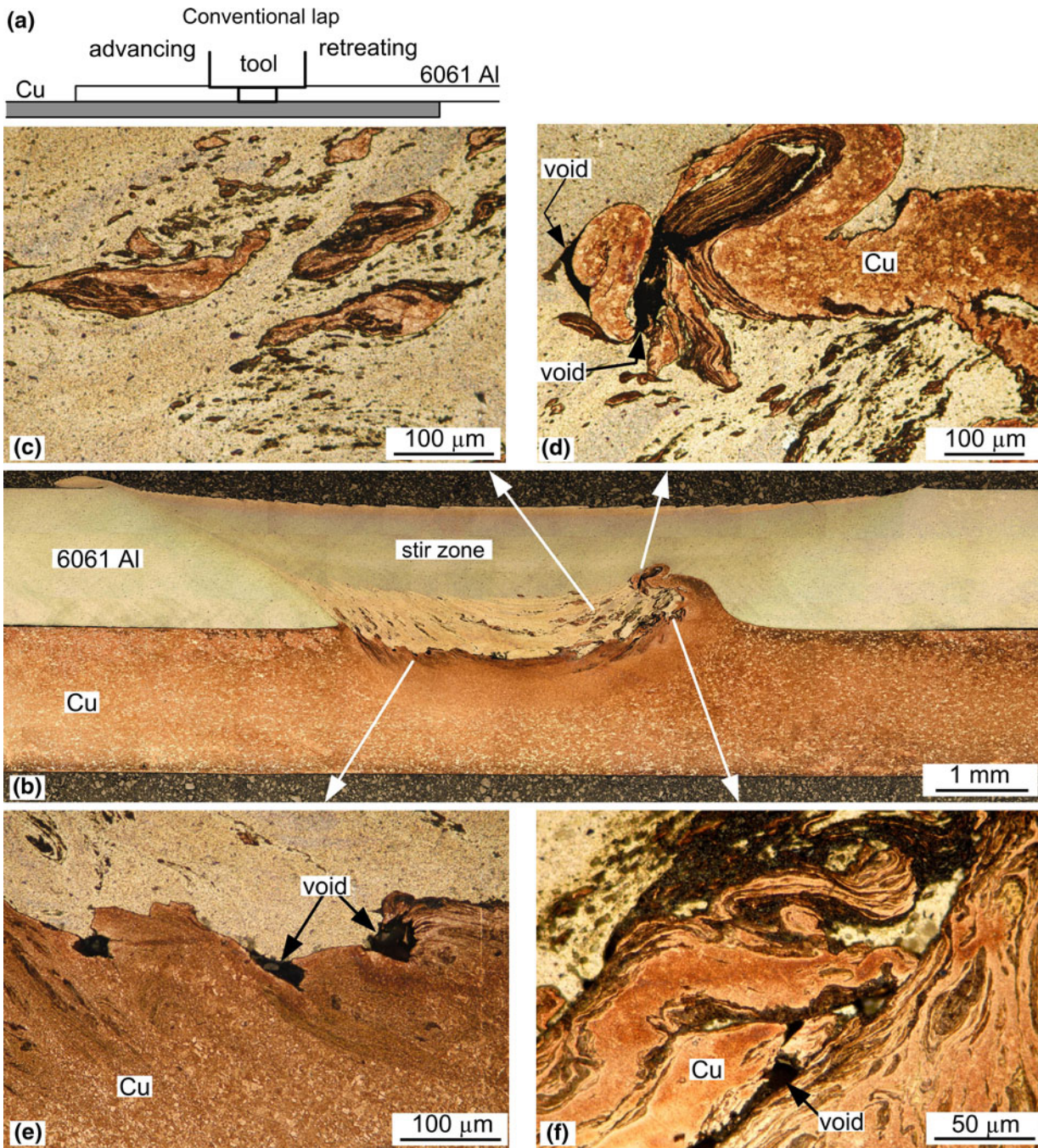


Fig. 12—Transverse cross section of conventional lap weld CL-2 (8 ipm or 203 mm/min): (a) joint design; (b) optical macrograph; (c) through (f) etched optical micrographs.

etches somewhat light brown in color, which again might suggest the presence of Cu particles and a solid solution of Al containing Cu. The upper portion of the stir zone in Cu is no longer pulled deep into the stir zone of the upper 6061 Al to interlock with it. More importantly, a channel exists between the lower left corner of the stir zone in Cu and the stir zone in 6061 Al. The presence of the channel is

consistent with the relatively low strength and ductility of the weld in tensile testing (Figure 5).

As compared with modified lap weld ML-1, insufficient plasticity of Cu seemed to be present during welding to make it flow and mix well with the stir zone of 6061 Al. It can be expected that the heat input and hence the plasticity are much lower at a higher

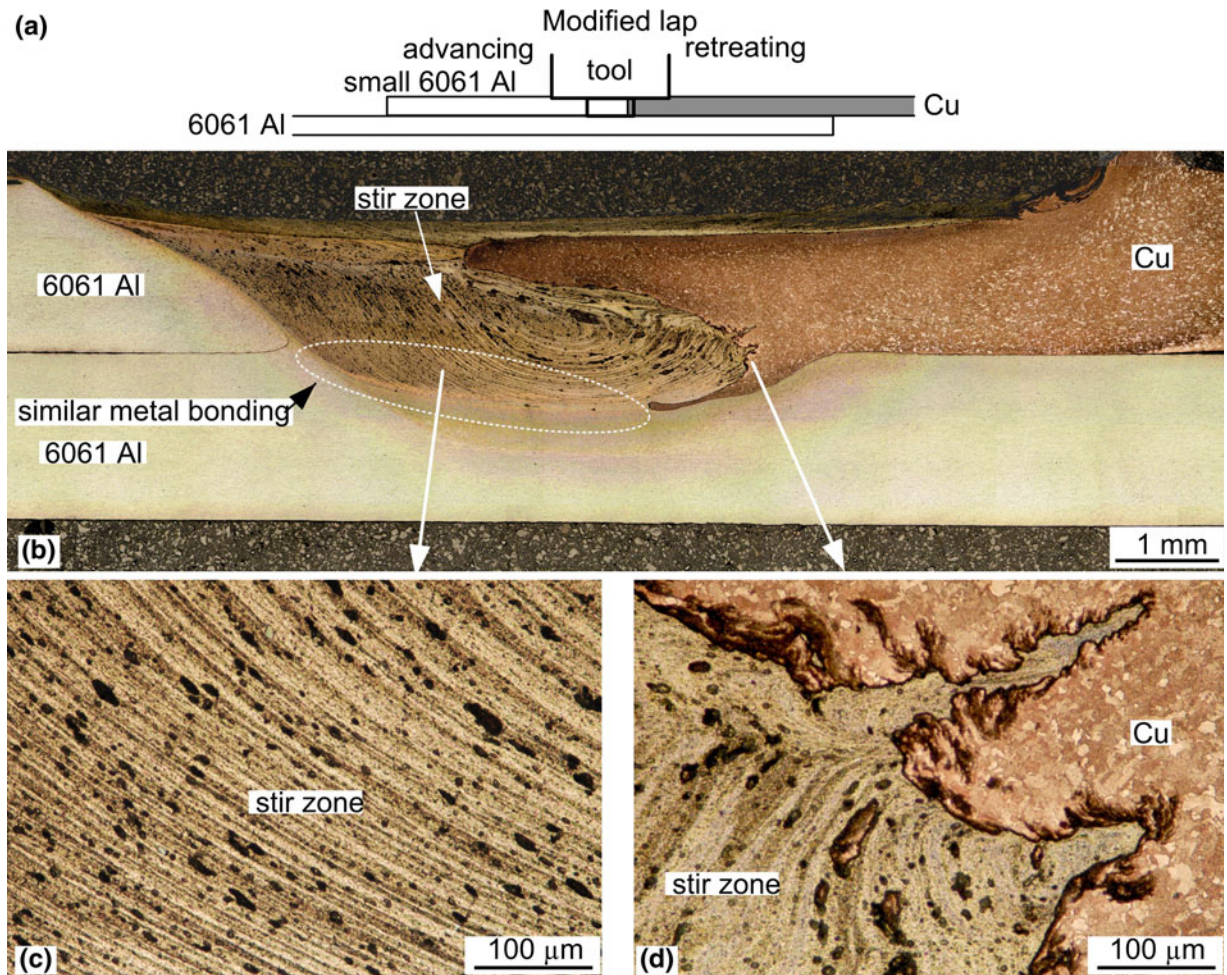


Fig. 13—Transverse cross section of modified lap weld ML-1 (1.5 ipm or 38 mm/min): (a) joint design; (b) optical macrograph; (c) and (d) etched optical micrographs.

travel speed of 203 mm/min vs 38 mm/min (8 ipm vs 1.5 ipm).

IV. CONCLUSIONS

Al-to-Cu lap FSW was studied by welding 1.6-mm sheets of 6061 Al and Cu. Conventional lap FSW was modified by butt welding a small piece of 6061 Al to Cu at the top, with a slight pin penetration into the 6061 Al at the bottom. Within the range of experimental conditions in the present study, the following conclusions can be drawn:

1. As in the recent study on Al-to-Mg lap FSW, modified lap FSW can significantly improve the weld quality in Al-to-Cu lap FSW.
2. At travel speeds up to 127 mm/min (5 ipm), the modified welds can be much better than the conventional lap welds—about twice higher in the joint strength and five to nine times higher in ductility. Voids are no longer present along the Al–Cu interface as in conventional lap welds, thus shifting the location of fracture in tensile testing from along the interface to through Cu.
3. At the relatively high travel speed of 203 mm/min (8 ipm), however, modified lap FSW may no longer be superior because of channel formation.

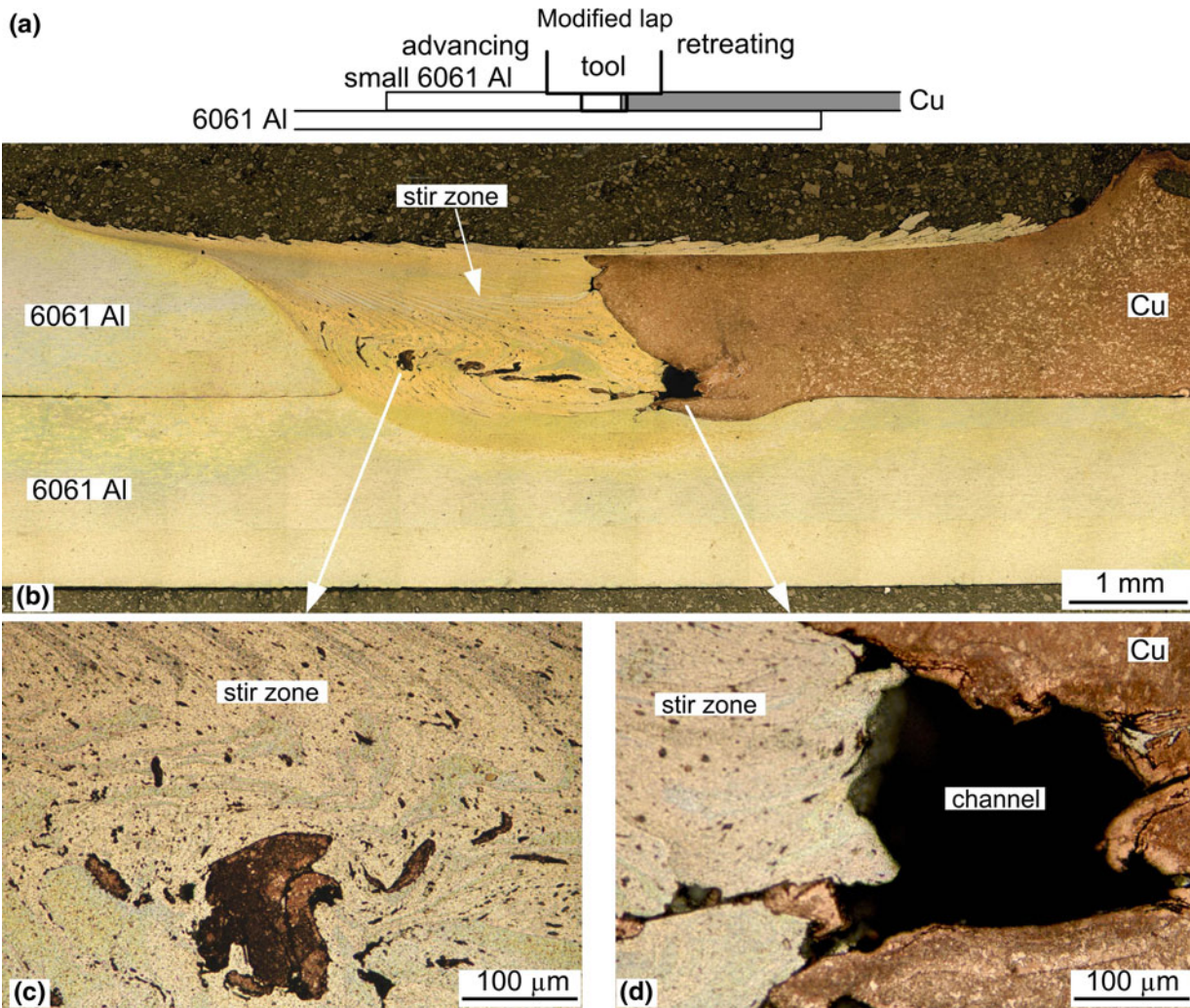


Fig. 14—Transverse cross section of modified lap weld ML-2 (8 ipm or 203 mm/min): (a) joint design; (b) optical macrograph; (c) and (d) etched optical micrographs.

ACKNOWLEDGMENTS

This work was supported by the Wisconsin Alumni Research Foundation of the University of Wisconsin-Madison. The authors would like to thank Dr. John H. Fournelle and Dr. Hiromi Konishi from the Department of Geoscience of the University of Wisconsin-Madison for their assistance in SEM and XRD experiments.

REFERENCES

1. C. Conrardy: *8th Int. Conf. on Trends in Welding Research*, Pine Mountain, GA, 2008.
2. K. Nakada and M. Ushio: *J. Jpn. Weld. Soc.*, 2002, vol. 71 (6), pp. 6–9.
3. W.M. Thomas, E.D. Nicholas, J.C. Needham, M.G. Murch, P. Tem-Plesmith, and C.J. Dawes: Patent Application No. 9125978.8, 1991.
4. H. Okamura and K. Aota: *National Conf. of the Japan Welding Society*, 2002.
5. A. Elrefaey, M. Takahashi, and K. Ikeuchi: *Welding in the World*, 2005, vol. 49 (3–4), pp. 93–101.
6. A. Elrefaey, M. Takahashi, and K. Ikeuchi: *J. High Temp. Soc.*, 2004, vol. 30 (5), pp. 286–92.
7. A. Abdollah-Zadeh, T. Saeid, and B. Sazgari: *Weldability and Mechanical Properties of Dissimilar Aluminum-Copper Lap Joints Made by Friction Stir Welding*, *Welding in South-East Asia: A Challenge for the Future*, International Welding Institute, Bangkok, Thailand, 2006.
8. A. Abdollah-Zadeh, T. Saeid, and B. Sazgari: *J. Alloys Compd.*, 2008, vol. 460, pp. 535–38.
9. P. Liu, Q. Shi, W. Wang, X. Wang, and Z. Zhang: *Mater. Lett.*, 2008, vol. 62, pp. 4106–08.
10. X. Wang, Z. Zhang, C. Da, and J. Li: *China Welding*, 2007, vol. 16 (1), pp. 57–62.
11. K. Savolainen, J. Mononen, T. Saukkonen, and H. Hanninen, *6th Int. Symp. on Friction Stir Welding*, Saint-Sauveur, Canada, 2006, pp. 1–10.
12. J. Ouyang, E. Yarrapareddy, and R. Kovacevic: *J. Mater. Process. Tech.*, 2006, vol. 172, pp. 110–22.
13. W.-B. Lee and S.-B. Jung: *Mater. Res. Innovat.*, 2004, vol. 8 (2), pp. 93–96.
14. A. Pietras: *Welding in the World*, 2005, vol. 49 (9), pp. 122–33.
15. G. Luan, C. Sun, H. Guo, and Y. Yu: *4th Int. Symp. on Friction Stir Welding*, Park City, UT, 2003, pp. 1–11.
16. L. Karlsson, E.-L. Bergqvist, and H. Larsson: *Welding in the World*, 2002, vol. 46, nos. 1,2, pp. 10–14.
17. R.D. Flores, L.E. Murr, and E.A. Trillo: *Electron Microsc.*, 1998, vol. 11, pp. 143–44.

18. L.E. Murr, E.A. Trillo, Y. Li, R.D. Flores, B.M. Nowak, and J.C. McClure: *Fluid Flow Phenomena in Materials Processing*, Eds., N. El-Kaddah, D.G.C. Robertson, S.T. Johansen, and V.R. Voller, TMS, Warrendale, PA, 1999, pp. 31–40.
19. American Society for Metals: *Binary Alloy Phase Diagrams vol. 1*, American Society for Metals, Metals Park, OH, 1986, p. 106.
20. Y.G. Kim, H. Fujii, T. Tsumura, T. Komazaki, and K. Nakada: *Mater. Sci. Eng. A*, 2006, vol. 415, pp. 250–54.
21. V. Firouzdor and S. Kou: *Weld. J.*, 2009, vol. 88, pp. 213s–224s.
22. V. Firouzdor and S. Kou: U.S. Patent Application No. 20110104515, 2009.
23. V. Firouzdor and S. Kou: *Metall. Mater. Trans. A*, 2010, vol. 41A (11), pp. 2914–35.
24. V. Firouzdor and S. Kou: *Metall. Mater. Trans. A*, 2010, vol. 41A (12), pp. 3238–51.